Langmuir

Letter

pubs.acs.org/Langmuir

Charged Nanoparticle Dynamics in Water Induced by Scanning Transmission Electron Microscopy

E. R. White, Matthew Mecklenburg, Brian Shevitski, S. B. Singer, and B. C. Regan*

Department of Physics and Astronomy & California NanoSystems Institute, University of California, Los Angeles, California 90095, United States

Supporting Information

ABSTRACT: Using scanning transmission electron microscopy we image ∼4 nm platinum nanoparticles deposited on an insulating membrane, where the membrane is one of two electron-transparent windows separating an aqueous environment from the microscope's high vacuum. Upon receiving a relatively moderate dose of $\sim 10^4$ e/nm^2, initially immobile nanoparticles begin to move along trajectories that are directed radially outward from the center of the field of view. With larger dose rates the particle motion becomes increasingly dramatic. These observations demonstrate that, even under mild imaging conditions, the *in situ* electron microscopy of aqueous environments can produce electrophoretic charging effects that dominate the dynamics of nanoparticles under observation.

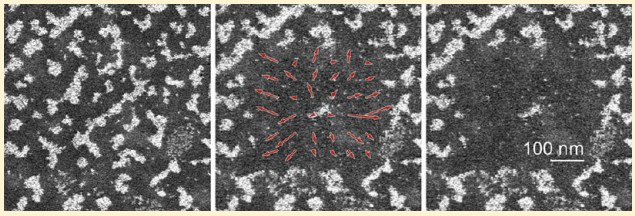

INTRODUCTION

At the cellular level most biological machinery is composed of highly charged molecules and macromolecular structures in aqueous solution.[1] Recent advances in the construction of environmental cells for use in transmission electron microscopes (TEMs) have made possible *in situ* experiments with high-vapor-pressure liquids such as water.[2−12] While the field is still in its infancy, such measurements clearly hold great promise for revealing the molecular basis of cellular function.[12−16] However, a key assumption for the most straightforward interpretations of many *in situ* TEM experiments is that the imaging technique is not substantially disturbing the system under observation. Here we present data demonstrating that, under imaging conditions that are not extreme, the electron beam in a TEM can produce dramatic dynamic effects even in an inert aqueous environment. As these effects arise from charging induced by the imaging beam, they represent both a potential obstacle and a possible tool for studies of biological and other processes governed by the Coulomb interaction in water.

Previous studies on liquid-filled cells have seen no noticeable beam effects in some cases, and sample modifications in others. Gold nanoparticles exposed to 10^6 e/nm^2 at 300 keV have been observed to move under the influence of a receding fluid boundary or random diffusion, but the heating, momentum transfer, and charging effects of the electron beam were all found to be negligible.[8] A STEM dose of 10^5 e/nm^2 at 200 keV applied to 10 nm gold particles labeling biological molecules also showed no remarkable effect on the sample,[13] but a dose ten times larger caused such particles to dissolve.[3] Two groups have used the electron beam to drive the gowth of nanoparticles from solutions of metalorganic precursors. In one case platinum nanocrystals were created with a dose of 10^5−10^6 e/nm^2 at 300 keV.[7] A similar experiment visualized the formation of lead sulfide nanoparticles, but dose information was not included in the report.[11]

Using scanning transmission electron microscopy (STEM), we image ∼4 nm platinum nanoparticles deposited on one of the windows of an electron-transparent, water-filled cell. An electron dose of $\sim 10^4$ e/nm^2 causes the nanoparticles to be expelled outward from the center of the field of view (FOV). Such small doses have not previously been noted to affect the system under observation in an aqueous environment.

EXPERIMENTAL METHODS

As in previous *in situ* aqueous TEM experiments,[2−8,13,14] the water is contained between two electron transparent membranes. The membranes are fabricated from 19 nm of Si_3N_4 and 850 nm of SiO_2 grown on a 200 μm thick Si(100) wafer.[6] A 20 μm × 300 μm hole is revealed in the silicon with a KOH etch and the membranes are subsequently thinned by an HF vapor etch to achieve electron transparency. In a scanning electron microscope (FEI Nova 600 Nanolab) equipped with a gas injection system, methylcyclopentadienyl (trimethyl) platinum vapor is decomposed with the electron beam to deposit nominally platinum nanoparticles measuring ∼4 nm in diameter on the membrane. Two silicon chips, one with nanoparticles deposited and one without, are glued together with epoxy (Hysol 1C-LV) around the outside edges, with a thin a layer of water separating the two chips. While the epoxy is setting micromanipulators are used to apply gentle pressure to the top chip to minimize the membrane separation. Although no spacer is used, the elevation variation produced by gold electrodes (not used in this experiment) and alignment markers on the bottom chip ensure that the chip spacing is greater than 130 nm. Under ambient conditions the

Received: December 8, 2011
Revised: February 8, 2012
Published: February 9, 2012

dx.doi.org/10.1021/la2048486 | Langmuir 2012, 28, 3695−3698

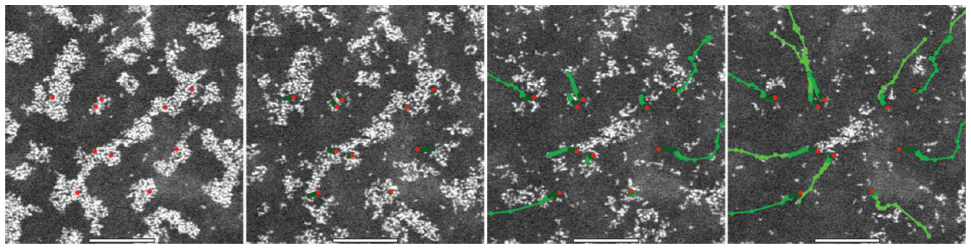

Figure 1. Time series of STEM images taken with a beam current of 57 pA and a 350 nm × 350 nm FOV (magnification 450 000×). The images are acquired ∼7 s apart, with time increasing to the right. The trajectories of 10 particles are shown with green tracks, with starting points denoted by red dots and the shade of green incrementing between frames. The scale bar in each image is 100 nm and the entire FOV is shown.

membrane spacing in a properly assembled device is less than a few hundred nanometers, as indicated by the window's lack of color when viewed in an optical microscope. (Thicker devices show brightly colored windows due to optical interference effects.) In the TEM's vacuum environment the water layer thickness likely changes as the membranes bulge outward.[17] A cell contains less than 0.1 nL of water.

We image the water-filled cells using an FEI Titan 80−300 TEM operated at 300 kV in scanning transmission electron microscopy (STEM) mode. Images measuring 512 pixels × 512 pixels are acquired with a dwell time of 1.3 μs per pixel, giving a frame acquisition time of 0.33 s. The spatial resolution is limited by the size of the pixel or the size of the electron beam after it has been spread by scattering in the sample (1−2 nm), whichever is larger.

RESULTS AND DISCUSSION

Figure 1 presents a time series of STEM images that span ∼30 s and show an area that contains ∼2000 nanoparticles at first (see Supporting Information, Movie SM1). The initially immobile nanoparticles begin to move after several seconds of imaging. As the exposure time increases the nanoparticle clusters break apart and individual nanoparticles leave the FOV. On some occasions clusters of nanoparticles appear to move over each other as they move away from the center (see Supporting Information, Movies SM1−4). Ten individual nanoparticles are tracked in Figure 1, with their trajectories shown in green. Generally the nanoparticles move radially outward from the center, and at times they appear to avoid clusters of other nanoparticles. The distance traveled per frame by each particle tends to increase with time, as indicated by the increasing separation between dots designating position measurements.

Half a minute of imaging under these relatively ordinary conditions decreases the density of nanoparticles in the FOV by an order of magnitude (Figure 2 a−b). In addition, the 'difference' image (Figure 2c) reveals that some particles in clusters neighboring the FOV, but not directly imaged, are also relocated. Light regions in the 'difference' image indicate that relocated nanoparticles come to rest as far as 50 nm from the FOV. Some nanoparticles may move much farther, as not all of the relocated material can be accounted for. We have observed displacements greater than 300 nm relative to the FOV boundary.

While the individual trajectories shown indicate that the particle flow is predominantly radial, particle image velocimetry (PIV) is used to ensure no selection bias. An image is divided into a 6 × 6 array of subimages, and each subimage is cross-correlated with the subsequent subimage of the same location. Averaging the cross-correlations over an entire time series and multiplying by the frame rate gives the average velocity of the particles in each subimage. These velocities are indicated with the vectors shown in Figure 2d. Deviations from purely radial motion are likely due to the tendency of nanoparticles to avoid

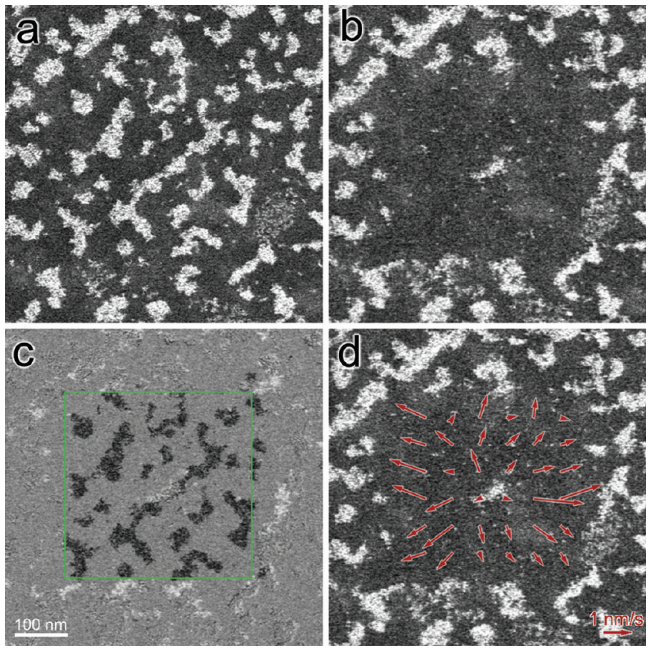

Figure 2. (a) The entire FOV of Figure 1 plus the surrounding area, immediately before the Figure 1 data was acquired. (b) The same region imaged immediately after the last frame of the data set. (c) 'Difference' image showing the result of subtracting the 'before' image from the 'after' image. Particles have relocated from the blacker regions to the lighter regions. The green box encloses the FOV from Figure 1. (d) Results of the PIV analysis.

large clusters of other particles. The longest vector corresponds to a velocity of 1.7 nm/s, while the shortest corresponds to 0.16 nm/s. In this PIV analysis motionless nanoparticles are counted while rapidly moving nanoparticles (when they cross a subimage boundary between frames) are not. Both effects tend to decrease the average velocities returned, so the PIV values are smaller than the typical velocity of a moving nanoparticle. For individual nanoparticles in this data set velocities greater than 150 nm/s are observed (see Figure 1). Above this value conclusive identification of a moving nanoparticle becomes progressively more difficult as the displacements between frames become comparable to the size of the FOV.

The rate at which the nanoparticles disperse can be controlled by adjusting either the exposed area (i.e., the microscope magnification) or the beam current. Thus we take the controlling variable to be the effective electron beam current density, where this density is defined as the beam current divided by the area of the STEM FOV. Larger current densities give increased dispersion rates. Figure 3 gives the

dx.doi.org/10.1021/la2048486 | *Langmuir* 2012, 28, 3695−3698

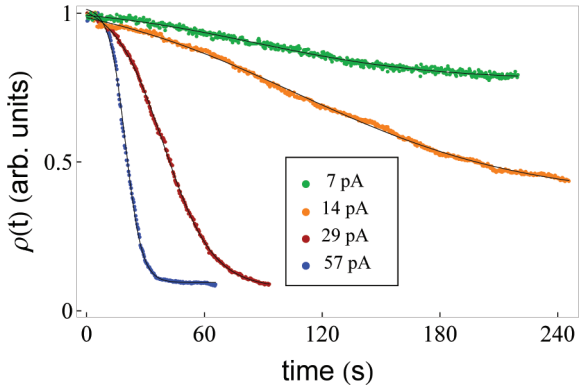

Figure 3. Density of nanoparticles in the full STEM FOV vs time for beam currents of 7 pA, 14 pA, 29 pA, and 57 pA. Each curve is normalized by its maximum value.

nanoparticle density in the full FOV as a function of time for various beam currents. The nanoparticle expulsion is more complete and more rapid for larger beam currents. As the data in Figure 3 show, system modifications can be tuned to occur over time scales ranging from seconds to minutes.[18] This level of control over the dynamical time scales is a key advantage for studies in TEMs that are limited to data acquisition at video rates.

The complex particle motions observed in these data sets depend upon forces that are fundamentally derived from the Coulomb interaction, but can be described in more specific terms. Adhesion, interparticle, van der Waals, solvation, depletion, double-layer, electrostatic, viscous, steric, frictional, lubrication, and Brownian forces all play a role in moving a particle from its initial location to hundreds of nanometers away.[19,20] A detailed explanation is beyond the scope of this work, but the relative importance of some force mechanisms can be ascertained from the data.

The individual nanoparticles undergo driven motion that is predominantly radial and observable over many seconds. Both observations indicate that the Brownian motion expected for free particles in solution is strongly suppressed; adhesion forces continue to play an important role even after the nanoparticles begin to move. A free particle in a fluid drifts randomly due to Brownian motion, with a mean-square displacement $\langle x^2 \rangle = 2kTt/\alpha$, where kT is the thermal energy, α is the drag coefficient, and t is the time. In the low Reynold's number limit appropriate for small particles Stoke's law gives a drag coefficient $\alpha = 6\pi\eta\delta$, where η is the dynamic viscosity of the surrounding fluid and δ is the particle radius. For 4 nm diameter free particles in water ($\eta = 10^{-3}$ N·s/m^2) a drift time of 0.33 s gives an expected mean-square displacement $(\langle x^2 \rangle)^{1/2} \sim 10$ μm, which is large compared to our FOV. Thus our Pt nanoparticles cannot be completely detaching from the membrane, because in this case single particles would not remain visible for more than one frame after their motion initiates. Random displacements between frames are smaller than the particle size, more than 3 orders of magnitude less than the expectation for free particles.

The small amplitude of the random drift implies a large effective drag coefficient. Hydrodynamic drag is known to be enhanced near a planar surface,[21,22] and previous *in situ* TEM measurements of the motion of ~10 nm gold nanocrystals in solution have seen strong substrate interactions and two-dimensional diffusion coefficients ~0.2 nm^2/s, similar to those seen here.[8] Using the same process recipe we deposited platinum nanoparticles on membranes and imaged them in the standard TEM high vacuum environment. These 'dry' samples showed no movement or morphology changes under identical beam conditions. Thus the presence of water, i.e., hydration, likely influences the adhesion and lubrication forces between the particles and the substrate and allows the particles to move.[19]

To explain the radial motion it is necessary to invoke long-range forces, i.e., ones that are appreciable on length scales comparable to the size of the FOV. We attribute the radially directed motion of the nanoparticles to electrophoresis caused by the charging of the membranes and the nanoparticles themselves. As is well-known, under the influence of a TEM's electron beam material can acquire net charge via Auger and secondary electron emission.[23] A uniform-charging model predicts a radial force based on symmetry considerations. In other words, to the extent that the material in the FOV charges uniformly under the influence of the electron beam, there will be an electric field with an in-plane component directed radially outward from the center of the FOV. Charged nanoparticles in the FOV will feel a force that decreases to zero at the center of the charged region (equivalent to the FOV in this model), which might explain why an anomalously large cluster of nanoparticles would be left in the center as in the last frame of Figure 1. (As this anomaly is not always observed, a local variation in the strength of the adhesive forces between the nanoparticles and the membrane could also be responsible.)

Debye screening limits the effective range of a nanoparticle's electromagnetic interactions. However, short-range forces explain the cluster-avoidance shown by some of the nanoparticles. Similarly charged surfaces with overlapping Debye layers are subject to an osmotic pressure that pushes the surfaces apart.[19] The deionized water used here would ideally have a Debye length of 1 μm, but exposure to epoxy and atmospheric gases during cell fabrication increases the concentration of ionic species. The Debye length is thus submicrometer, but still sufficiently lengthy that significant nanoparticle interaction occurs. To the extent that the Debye length is short, incomplete screening arises because the nanoparticles remain attached to the membrane. Unscreened fields penetrate the half-space delineated by the membrane-water boundary, which allows for charge interactions between particles and between particles and the membrane itself.

We have considered other possible explanations for the large-scale motion of the nanoparticles. While the fluid cells often contain air pockets, vapor generates obvious contrast compared to the water.[6] No bubbles were near the FOV for the data reported here, thus interfacial phenomena, e.g., marangoni convection, can be ruled out. Another possibility is thermally driven diffusion, or thermophoresis,[24] caused by the heat deposited by the STEM beam. The STEM beam produces a temperature increment above ambient in the center of the FOV which is given by[25]

$$\Delta T \simeq \frac{I_b}{2\pi^2 e\kappa}\frac{dE}{dx}\ln\left(\frac{\pi}{2}\frac{a}{d}\right) \quad (1)$$

To estimate the temperature change ΔT we take the beam current $I_b = 57$ pA, the energy loss rate per electron $dE/dx = 0.04$ eV/nm in water, and the governing thermal conductivity to be that of water, $\kappa = 0.5$ W/m·K.[8] For a FOV with dimension $a = 350$ nm and a probe with dimension $d = 1$ nm,

dx.doi.org/10.1021/la2048486 | *Langmuir* 2012, 28, 3695−3698

these values give a temperature increment $\Delta T \simeq 0.001$ K. The small size of the implied temperature gradient indicates that heating by the electron beam is not responsible for driving the nanoparticles from their initial positions.

CONCLUSION

In conclusion, we have presented here the first TEM observations and analysis of charge-induced nanoparticle dynamics in solution. The nanoparticles acquire charge as a direct consequence of exposure to the imaging beam. Operating in STEM mode, a user has detailed control over the dose, dose rate, and exposed area. Since these parameters dictate the magnitude and location of the charging, STEM experiments can probe Coulomb-derived interactions in aqueous solution with unprecedented spatial resolution. These observations are especially relevant for *in situ* TEM studies of functional biomolecules and biostructures, where charge interactions are known to play a dominant role.

ASSOCIATED CONTENT

Supporting Information

Four movie files SM1−SM4 showing Pt nanoparticle expulsion from the 350 nm × 350 nm STEM FOV, with beam currents of 57, 29, 14, and 7 pA, respectively. The scale bar is 100 nm. This material is available free of charge via the Internet at http://pubs.acs.org.

AUTHOR INFORMATION

Corresponding Author

*E-mail: regan@physics.ucla.edu.

Notes

The authors declare no competing financial interest.

ACKNOWLEDGMENTS

The authors acknowledge the Electron Imaging Center for NanoMachines supported by the NIH (1S10RR23057) and the CNSI at UCLA. Acknowledgment is made to the donors of The American Chemical Society Petroleum Research Fund for support of this research. This work was also supported by NSF CAREER grant DMR 0748880 and NSF HRD00603239 (CAMP).

REFERENCES

(1) Gelbart, W.; Bruinsma, R.; Pincus, P.; Parsegian, V. DNA-Inspired Electrostatics. *Phys. Today* **2000**, *53*, 38.

(2) Williamson, M. J.; Tromp, R. M.; Vereecken, P. M.; Hull, R.; Ross, F. M. Dynamic microscopy of nanoscale cluster growth at the solid-liquid interface. *Nat. Mater.* **2003**, *2*, 532−6.

(3) de Jonge, N.; Poirier-Demers, N.; Demers, H.; Peckys, D. B.; Drouin, D. Nanometer- resolution electron microscopy through micrometers-thick water layers. *Ultramicroscopy* **2010**, *110*, 1114−9.

(4) Grogan, J.; Bau, H. The Nanoaquarium: A Platform for In Situ Transmission Electron Microscopy in Liquid Media. *J. Microelectromech. Syst.* **2010**, *19*, 885−894.

(5) Radisic, A.; Ross, F. M.; Searson, P. C. In Situ Study of the Growth Kinetics of Individual Island Electrodeposition of Copper. *J. Phys. Chem. B* **2006**, *110*, 7862−8.

(6) White, E.; Mecklenburg, M.; Singer, S.; Aloni, S.; Regan, B. Imaging Nanobubbles in Water with Scanning Transmission Electron Microscopy. *Appl. Phys. Exp.* **2011**, *4*, 055201.

(7) Zheng, H.; Smith, R. K.; Jun, Y.-W.; Kisielowski, C.; Dahmen, U.; Alivisatos, A. P. Observation of single colloidal platinum nanocrystal growth trajectories. *Science* **2009**, *324*, 1309−12.

(8) Zheng, H.; Claridge, S. A.; Minor, A. M.; Alivisatos, A. P.; Dahmen, U. Nanocrystal diffusion in a liquid thin film observed by in situ transmission electron microscopy. *Nano Lett.* **2009**, *9*, 2460−5.

(9) Klein, K. L.; Anderson, I. M.; de Jonge, N. Transmission electron microscopy with a liquid flow cell. *J. Microsc.* **2011**, *242*, 117−23.

(10) Grogan, J.; Rotkina, L.; Bau, H. In situ liquid-cell electron microscopy of colloid aggregation and growth dynamics. *Phys. Rev. E* **2011**, *83*, 1−5.

(11) Evans, J. E.; Jungjohann, K. L.; Browning, N. D.; Arslan, I. Controlled growth of nanoparticles from solution with in situ liquid transmission electron microscopy. *Nano Lett.* **2011**, *11*, 2809−13.

(12) de Jonge, N.; Ross, F. M. Electron microscopy of specimens in liquid. *Nat. Nanotechnol.* **2011**, 1−10.

(13) de Jonge, N.; Peckys, D. B.; Kremers, G. J.; Piston, D. W. Electron microscopy of whole cells in liquid with nanometer resolution. *Proc. Natl. Acad. Sci. U.S.A.* **2009**, *106*, 2159−64.

(14) Liu, K.-L.; Wu, C.-C.; Huang, Y.-J.; Peng, H.-L.; Chang, H.-Y.; Chang, P.; Hsu, L.; Yew, T.-R. Novel microchip for in situ TEM imaging of living organisms and bio-reactions in aqueous conditions. *Lab Chip* **2008**, *8*, 1915−21.

(15) Dukes, M. J.; Peckys, D. B.; de Jonge, N. Correlative Fluorescence Microscopy and Microscopy of Quantum-Dot-Labeled Proteins in Whole Cells in Liquid. *ACS Nano* **2010**, *4*, 4110−4116.

(16) Peckys, D. B.; de Jonge, N. Visualizing gold nanoparticle uptake in live cells with liquid scanning transmission electron microscopy. *Nano Lett.* **2011**, *11*, 1733−8.

(17) Creemer, J.; Santagata, F.; Morana, B.; Mele, L.; Alan, T.; Iervolino, E.; Pandraud, G.; Sarro, P. An all-in-one nanoreactor for high-resolution microscopy on nanomaterials at high pressures; 2011 IEEE 24th International Conference on Micro Electro Mechanical Systems (MEMS); pp 1103−1106.

(18) We are not able to establish a threshold below which charging effects are completely eliminated. Even successive images acquired with a total dose of $\sim 10^3$ e/nm^2 show subtle nanoparticle movement in this sample.

(19) Israelachvili, J. *Intermolecular and Surface Forces*; Acedemic Press Inc.: London, 2011.

(20) Min, Y.; Akbulut, M.; Kristiansen, K.; Golan, Y.; Israelachvili, J. The role of interparticle and external forces in nanoparticle assembly. *Nat. Mater.* **2008**, *7*, 527−38.

(21) Kazoe, Y.; Yoda, M. Measurements of the near-wall hindered diffusion of colloidal particles in the presence of an electric field. *Appl. Phys. Lett.* **2011**, *99*, 124104.

(22) Holmqvist, P.; Dhont, J.; Lang, P. Anisotropy of Brownian motion caused only by hydrodynamic interaction with a wall. *Phys. Rev. E* **2006**, *74*, 1−5.

(23) Cazaux, J. Correlations between ionization radiation damage and charging effects in transmission electron microscopy. *Ultramicroscopy* **1995**, *60*, 411−425.

(24) Duhr, S.; Braun, D. Why molecules move along a temperature gradient. *Proc. Natl. Acad. Sci. U.S.A.* **2006**, *103*, 19678−82.

(25) Kohl, H.; Rose, H.; Schnabl, H. Dose-rate effect at low temperatures in FBEM and STEM due to object-heating. *Optik* **1981**, *58*, 11−24.